Aconitic acid recovery from sugar-cane stillage: from the modelling of the anion-exchange step to the conception of a novel combined process

Jenny Wu-Tiu-Yen, Marie-Laure Lameloise, Arnaud Petit, Richard Lewandowski, B. Broyart, Claire Fargues

▶ **To cite this version:**

Jenny Wu-Tiu-Yen, Marie-Laure Lameloise, Arnaud Petit, Richard Lewandowski, B. Broyart, et al.. Aconitic acid recovery from sugar-cane stillage: from the modelling of the anion-exchange step to the conception of a novel combined process. Separation Science and Technology, 2021, 56 (10), pp.1752-1768. 10.1080/01496395.2020.1795677 . hal-03640629

HAL Id: hal-03640629

https://agroparistech.hal.science/hal-03640629

Submitted on 13 Apr 2022

HAL is a multi-disciplinary open access archive for the deposit and dissemination of scientific research documents, whether they are published or not. The documents may come from teaching and research institutions in France or abroad, or from public or private research centers.

L'archive ouverte pluridisciplinaire **HAL**, est destinée au dépôt et à la diffusion de documents scientifiques de niveau recherche, publiés ou non, émanant des établissements d'enseignement et de recherche français ou étrangers, des laboratoires publics ou privés.

Aconitic acid recovery from sugar-cane stillage: from the modelling of the anion-exchange step to the conception of a novel combined process

Wu-Tiu-Yen J.[b], Lameloise M.-L.[a], Petit A.[b], Lewandowski R.[a], Broyart B.[a], Fargues C.[a*]

[a] *Université Paris-Saclay, INRAE, AgroParisTech, UMR SayFood, 91300, Massy, France*

[b] *eRcane, 97494 Sainte-Clotilde Cedex France*

* Corresponding author:
Claire Fargues, AgroParisTech, 1 avenue des Olympiades, 91744 Massy cedex, France
claire.fargues@agroparistech.fr

Aconitic acid recovery from sugar-cane stillage: from the modelling of the anion-exchange step to the conception of a novel combined process

ABSTRACT

Sugarcane stillage is rich in tri-carboxylic aconitic acid. To study its purification through anion-exchange, selectivity coefficients between aconitate and the major competing minerals were determined on a weak-base resin for different pH. Simulation of solutes separation in column, using mass conservation equations and equilibrium theory, confirmed that resin in sulfate form and pH = 4.5 led to the best separation performances, and showed that a preliminary chloride removal up to 0.5 g L^{-1} was the most profitable to increase the ionic exchange capacity for aconitic acid. Demineralization of a real stillage by conventional electrodialysis followed by the optimized ion-exchange step, led to an aconitic acid-rich extract.

Keywords: sugarcane stillage; aconitic acid; ion-exchange; low-pressure chromatography; electrodialysis

Nomenclature and units

BV = resin Bed Volume (in liter of resin or L_R)

C_i = mass concentration of i in solution (g L^{-1})

C_{i0} = initial mass concentration of i in solution, for batch experiments (g L^{-1})

$C_{F\,i}$ = mass concentration of i in the column feed (g L^{-1})

D_{ax} = axial dispersion coefficient in the column (m^2 s^{-1})

DM = dry matter content (% w/w)

ε = Resin bed porosity (-)

FB = Free Base form

K_x i/j = Rational selectivity coefficient, considering i/j pair of anions (-)

L = column length (m)

m = resin dry mass in the column or in the closed flasks (g_R)

$N = \sum[i]$ (eq L^{-1})

P = aconitic acid purity with respect to DM (% w/w)

P_{app} = aconitic acid apparent purity with respect to global anions content analyzed in the solution (% w/w)

q_i = mass retention capacity of solute i on the resin (g L_R^{-1} or g g_R^{-1})

$q_{max\,Aaco}$ = maximal mass retention capacity of aconitic acid on the resin (g L_R^{-1} or g g_R^{-1})

$q_{tot} = \sum[R-i]$ = total ionic exchange capacity of the resin (eq L_R^{-1} or eq g_R^{-1})

R_{Aaco} = Aconitic acid recovery rate in elution fractions (%)

u = linear velocity of the fluid assumed uniform on a section of the column (m s^{-1})

V = volume of solution for equilibrium measurements in closed flasks (L)

V_0 = void volume in the column (L)

V_{si} = stoichiometric or average breakthrough volume for the solute i (L)

V_{sat} = saturation volume passed until having at the column outlet $C = 0.95\ C_F$ (L)

x_i = ionic fraction of solute i in solution (-)

y_i = ionic fraction of solute i in the resin (-)

Y_{Aaco} = Aconitic acid regeneration yield during elution step in column (%)

$Y_{Sat\ Aaco}$ = Aconitic acid yield during saturation phase (%)

[i] = solute i concentration in solution (eq L^{-1})

[R-i] = solute i concentration in resin phase (eq L_R^{-1} or eq g_R^{-1})

1. Introduction

Since 2000 and due to the instability of the world sugar market, sugar producers intend to better valorize their by-products by extracting high-value solutes. Regarding cane sugar industry, several by-products (especially molasses and stillage) are rich in valuable organic compounds including carboxylic acids, phenol derivatives, amino acids, proteins and coloring matters[1]. Aconitic acid, a tricarboxylic acid present as cis- or trans- isomer (Figure 1), is one of the prevalent organic molecules[2]. Its trans- form is predominant and the cis- one is unstable, leading to trans.

Aconitic acid has a great potential in a number of areas: it can be used as acidulant or umami flavor enhancer in food[3]. It is also currently considered with great interest for its antibacterial, anti-inflammatory, anti-tumoral or herbicide properties[4-6] and its use for the synthesis of vinyl polymers[7, 8] or as precursor for itaconic acid production[9, 10] has been described. Eventually, it belongs to the second class of the building block chemicals[11] due to its unsaturated tricarboxylic acid structure. Today, it is obtained chemically from citric acid by dehydration[12] and its production currently stands at about 400 kg/year.

It was shown that its concentration could reach 2 g L^{-1} in sugarcane juices and as much as 5% (% Dry Matter, w/w) in cane molasses[13]. Its recovery from these by-products has been studied by liquid-liquid extraction (mainly with tributylphosphate), or salt precipitation [2, 14, 15]. However, concern for more environment friendly processes such as ion-exchange and membrane techniques has embraced the sector of agroindustry by-products valorization, both for solutes extraction[16, 17] and water recovery[18]. They follow

the same trend as recent organic acids production schemes from microbial fermentation broth, generally targeted around combination of membrane, ion-exchange membrane, adsorption and/or ion exchange chromatography techniques[19-23], sometimes including *in situ* recovery[24, 25]. But far from the issue of an optimized and targeted fermentation, purification processes applied on by-products have to face specific challenges due to composition fluctuations and low purity of the target solute to valorize. Some studies exist on aconitic acid extraction by anion-exchange from cane molasses or juices[2, 26, 27], but the data obtained (capacity information, etc) do not allow scaling up, neither performances prediction for different compositions. A report[28] on 2007 sugarcane campaign in La Réunion confirmed that there was about 5% of aconitic acid (% Dry Matter, w/w) in local sugarcane distilleries stillage, a waste representing a potential resource of more than 1200 t of aconitic acid /year, and up to now most often discharged in the sea. Aconitate is there much diluted and only represents 20% (w/w) of the global anion content (Table 1), the remainder anions being composed of carboxylates including lactate, acetate and citrate, in addition to minerals. Specificity and capacity are therefore key parameters for its sustainable extraction and purification processes.

A preliminary study[29, 30] on cane stillage from Rivière du Mât distillery (Saint-Benoît, La Réunion, France) has resulted in the selection through batch mode experiments of a weak anionic resin (LEWATIT ® S4528), used in sulfate form. Separation in column led to separate aconitic acid from other less retained carboxylic acids. But high contents of minerals still remained in the eluate obtained, with an insufficient purity only up to 14% (w/w). A comprehensive evaluation of the efficiency of this step and its improvement appeared necessary. The ambition of this work is to provide for the first time generic data enabling scaling of the anion-exchange step, for the different aconitate forms (H_2Aaco^- and $HAaco^{2-}$ at stillage pH values studied), in competition with the major minerals present

in the stillage (chloride and sulfate) on the preselected resin. Therefore batch mode experiments were run and the ion-exchange coefficients obtained used in a model of multi-components ion-exchange in column. The behavior of a synthetic solution containing only aconitic acid, chloride and sulfate was studied at two pH (pH = 4.5 (natural pH of the stillage) and pH = 3.6 (mainly monovalent aconitate form (Figure 2)) in order to evaluate the influence of the aconitate valence on the resin selectivity. Breakthrough simulations with the adjusted parameters set were then run to predict the potential capacity gain for aconitic acid if a preliminary desalting step took place. Since it had been shown that conventional homopolar electrodialysis (ED) was an efficient pre-treatment step to separate organics from salts [16, 31-33], a combined ED / Anion-exchange separation process was evaluated for the purification of a real sugar cane stillage.

2. Methods

2.1. Resin, chemicals and solutions

The weak base macroporous resin LEWATIT® S4528 selected from previous work[30] was used and purchased from Lanxess (Courbevoie, France). Its physical properties are given in Table 2. In the pH range investigated (2.5 - 5.6) weak base sites of the anionic resin are fully ionized.

NaCl was purchased from Fisher Chemicals (Illkirch, France), trans-aconitic acid 98 % from Sigma Aldrich (Saint-Louis, MO, USA), Na_2SO_4, H_2SO_4 and HCl 37 % from Panreac (Barcelone, Spain) and NaOH from VWR Prolabo (Leuven, Belgium).

The study was run with different lots of sugarcane stillage supplied by Rivière du Mât distillery. Once collected, stillage was micro-filtered right away on a TIA filtration system (Bollène, France) equipped with 0.14 µm ceramic membranes and kept frozen until

further experiments. To compensate for the variability of the lots (DM between 4 to 10.5 %), stillage was standardized by adjusting the concentration of the major compounds so as to obtain a standard composition (Table 3). It was checked through the analyses that both cis- and trans-aconitic acid had the same behavior in the present study (same breakthrough). Consequently, they were considered as a single species (their concentrations were added) and C_{Aaco} set at 5 g L^{-1} by addition of trans-aconitic acid. Stillage purity in aconitic acid was then $P \approx 6$ % (w/w), and its pH about 4.5. To study pH influence on the chromatographic separation, for some of the experiments standard stillage had to be acidified until pH 3.6 while keeping the anion content unchanged. This was achieved by cation-exchange with Amberlite 252 resin in H^+ form (Dow Chemical). A given volume of acidified stillage was further mixed with the un-acidified one in order to reach the required pH. The composition of this solution was assessed by HPIC analysis to ensure that the resulting anion concentrations conform to the standard composition (table 3). Overall the concentration of the solution after pH correction being slightly lower than the standard composition, it was adjusted by addition of the major compounds.

In order to evaluate ion-exchange mechanism between the major ion species contained in stillage, a synthetic solution was also studied. It only contained trans-aconitate, chloride and sulfate anions, at the concentrations of the standard stillage (Table 3). Its natural pH being about 2, between 8 and 12 mL of 5 M NaOH solution was added to 1 L solution to reach the targeted pH of 3.6 or 4.5.

2.2. Analyses

Anions (organic and minerals) were quantified by High Performance Ionic Chromatography (HPIC) on a Dionex ICS-3000 equipment (Courtaboeuf, France) equipped with a DP ICS-3000 pump, an AS ICS-3000 auto-sampler (4°C) and a

conductimetric ICS-3000 CD detector. The IonPac AS11-HC column (250 mm x 4 mm i.d., 10 µm particle size, Dionex Courtaboeuf, France) was used and heated at 30°C. The mobile phases used are (A) NaOH 0.1 mol L^{-1} and (B) ultra-pure milli-Q water. Flow-rate was 1 mL min^{-1}. After 1 min of 2% A, A increased from 2 to 4% in 9 min, then from 4 to 30% in 15 min, and finally from 30% to 60% in 10 min; then it returned to 2% during 2 min. Global analysis duration was 38 min. With this method, trans- and cis-aconitic acid could be distinguished.

Stillage and breakthrough samples obtained during the adsorption phase on the column were diluted 100 times before analysis, and samples from column elution, 200 times. Before analysis, they were all filtered on a «Syringe Filter» with a porosity of 0.45 µm.

Based on repeatability tests, precision (relative standard deviation (RSD)) of about 10% was evaluated for aconitic acid and 5% for other solutes.

Dry Matter (%) was measured for some of the samples in order to determine aconitic acid purity *P* (w/w). Therefore a vacuum oven (70 °C, 0.1 bar) from Vaciotem (Selecta, Barcelone, Spain) was used. Between 2 g and 10 g of sample was introduced and mixed homogenously with about 30 g of sea sand from Panreac (Barcelone, Spain), previously dried and weighted. It was let to dry in the vacuum oven during 18 hours and Dry Matter calculated by weight difference after 30 minutes cooling in a desiccator.

2.3. Selectivity coefficients and resin capacity determination

The ion-exchange reaction between two anions of equivalent charge can be written according to the mass action law. For H_2Aaco^- /Cl^- exchange on a resin R, it gives:

$$R\text{-}Cl + H_2Aaco^- \leftrightarrows R\text{-}H_2Aaco + Cl^- \quad (1)$$

The corresponding rational selectivity coefficient is defined as:

$$K_x\ H_2Aaco^-/Cl^- = \frac{y_{H_2Aaco^-}}{x_{H_2Aaco^-}}\ \frac{x_{cl^-}}{y_{Cl^-}}\ = \frac{(1-y_{Cl^-})}{(1-x_{Cl^-})}\ \frac{x_{Cl^-}}{y_{Cl^-}} \qquad (-) \qquad (2)$$

with

$x_i = \frac{[i]}{N}$ = ionic fraction of solute i in solution (-)

$y_i = \frac{[R-i]}{q_{tot}}$ = ionic fraction of solute i in the resin (-)

$[i]$ = solute i concentration in solution (eq L^{-1}) = (solute i valence).C_i (g L^{-1}) / M_i

[R-i] = solute i concentration in resin phase (eq L_R^{-1} or eq g_R^{-1} depending if resin quantity is expressed in volume (L_R) or dry mass (g_R))

$N = \sum[i] = [Cl^-] + [H_2Aaco^-]$ (eq L^{-1})

$q_{tot} = \sum[R-i] = [R-Cl] + [R-H_2Aaco]$ = total ionic exchange capacity of the resin (eq L_R^{-1} or eq g_R^{-1})

$\sum x_i = 1 \qquad \text{and} \qquad \sum y_i = 1$

Exchange between anions of different valences (for example H_2Aaco^-/SO_4^{2-}) is written as:

$$R_2\text{-}SO_4 + 2\ H_2Aaco^- \leftrightarrows 2(R\text{-}H_2Aaco) + SO_4^{2-} \qquad (3)$$

and its corresponding rational selectivity coefficient is:

$$K_x\ H_2Aaco^-/SO_4^{2-} = \frac{y^2_{H_2Aaco^-}}{x^2_{H_2Aaco^-}}\ \frac{x_{SO_4^{2-}}}{y_{SO_4^{2-}}}\ = \frac{\left(1-y_{SO_4^{2-}}\right)^2}{\left(1-x_{SO_4^{2-}}\right)^2}\ \frac{x_{SO_4^{2-}}}{y_{SO_4^{2-}}}\ (-) \qquad (4)$$

Determination of the equilibrium $y_i = f(x_i)$ of the solute i, exchanged with solute j on the resin, allows the rational selectivity coefficient of the anion pair i/j, K_x i/j to be estimated, according to a least square non-linear minimization method.

Equilibria were achieved in closed flasks at 25°C. About 1 g of wet resin (precisely weighted) in free-base form was added to V = 50 mL of a mixture containing trans-aconitic acid and either Na_2SO_4 or NaCl at different initial concentrations C_{i0} (g L^{-1}). Before measurement of C_{i0}, initial pH was adjusted below 2 with either 0.5 M H_2SO_4 or 1 M HCl so as to ensure after equilibrium, a pH below 3.3, for which there is no divalent aconitate. For some of the experiments with sulfate, equilibrium pH was in the range 4 – 5.6, close to the natural pH of the stillage, for which divalent and monovalent aconitate forms are in equivalent proportions.

After stirring (48 hours), equilibrium was reached and concentrations C_i (g L^{-1}) were measured by HPIC. pH was also controlled allowing the contribution of each ionized state of solute i to be calculated. Taking account of the valence of each of these states, global [i] (eq L^{-1}) was calculated for each species, and consecutively N that considers all the species, and as a result x_i.

In relation with the known dry mass m of resin in the flask, mass balance allowed the solid-phase concentration of each species q_i (g g_R^{-1}) in equilibrium with C_i to be deduced:

$$q_i = \frac{(C_{i0} - C_i)\,V}{m} \qquad (5)$$

Therefore, the ratio -dry/wet- resin mass had previously been measured precisely: after preconditioning of the resin, it was filtered (0.45 μm) under vacuum so as to remove most of the liquid. A sample of this wet resin was weighted and dried (104 °C during 24 h), in order to obtain each time the given ratio -dry/wet- resin masses used to determine m. For each flask and ion pairs, taking account of the valence of the ions exchanged (as for [i]), calculation of the ionic concentration of each solute in the resin [R-i] (eq g_R^{-1}) was obtained from q_i , and consequently q_{tot} (eq g_R^{-1}) and y_i could be calculated.

In order to confirm the value of q_{tot}, the total ion-exchange capacity of the resin, acid/base titration of the resin was made [34, 35].

2.4. Column experiments and model development

2.4.1. Experimental procedure

Breakthrough of the main anionic components was studied through loading or saturation phase, where the column was fed with synthetic solution or standard stillage until resin saturation.

Experiments were run at room temperature on LEWATIT® S4528 previously conditioned in chloride or sulfate form, using a 40 cm x 1.5 cm i.d. Omnifit Solvent Plus glass column (Gilson, Villiers-Le-Bel, France) equipped with a peristaltic pump Minipuls 3 and a fraction collector FC 204 (both from Gilson, Villiers-Le-Bel, France). The column was full of liquid and a piston was used to evenly distribute the solution on the resin top surface (leaving a volume of liquid over the resin bed less than 1 mL). Bed height and consequently Bed Volume (BV, in resin liter, L_R) were then measured. For each of the resin forms tested, BV was about 60 mL. After each experiment, the resin was recovered and its dry mass weighed after drying at 104°C during 24 h. The average resin dry mass/Bed Volume (or apparent density) obtained were about 240 $g_R\ L_R^{-1}$ for both sulfate and chloride forms and 324 $g_R\ L_R^{-1}$ (FB) for its free-base form, half that given by the supplier (Table 2).

During saturation, at least 20 BV of solution was percolated downward at a flow-rate of 2 BV h^{-1}, after what the resin bed was rinsed at the same flow-rate with distilled water (2 BV). Fractions were collected at the column outlet for pH measurement and anions analyses. Elution step then took place upward at 1 BV h^{-1} with 10 BV of a regeneration solution: either, H_2SO_4 0.25 M to recover resin in sulfate form or HCl 0.5 M to recover it

in chloride form. In the fractions collected all along the step, pH was measured and anions analyzed.

2.4.2. Calculations

Saturation phase

- The mass center of the solute i breakthrough curve or stoichiometric breakthrough volume V_{si} (L) was calculated as

$$V_{Si} = \frac{\int_0^{C_{Fi}} V dC_i}{C_{Fi}} \quad (6)$$

With C_{Fi} = mass concentration of i in the column feed (g L^{-1}).

- Mass retention capacity of solute i in the column can then be deduced according to the solute mass balance, between solute feed and outlet until V_{si}:

$$q_i = \frac{C_{Fi}(V_{Si} - V_0)}{m} \quad (g\ g_R^{-1}) \quad (7)$$

Where

V_0 = void volume (L), including the extra-column volume contribution (pipes and other dead volumes of the equipment) plus the resin bed porosity estimated at 50% of BV, giving a total V_0 about 0.8 BV.

m = resin dry mass in the column (g_R).

- Aconitic acid yield ($Y_{Sat\ Aaco}$) during saturation phase was estimated relatively to the minimal passed V_{sat} until reaching $C = 0.95C_F$ at the column outlet; it accounts for Aaco loss, due to breakthrough spreading:

$$Y_{Sat\ Aaco} = 100\frac{V_{SAaco}}{V_{sat\ Aaco}} \quad (\%) \quad (8)$$

Elution step

During elution, aconitate is expected to separate in a certain extent from other retained anions. Its performances were estimated by:

- Aconitic acid regeneration yield, Y_{Aaco}, which is the ratio between the quantity recovered through elution and that adsorbed during saturation:

$$Y_{Aaco} = 100 \frac{m_{Aaco\ tot\ recovered}}{m_{Aaco\ retained}} \ (\%) \qquad (9)$$

With

$m_{Aaco\ tot\ recovered}$ = global mass of aconitic acid recovered in the elution samples all along the elution step (g)

$$m_{Aaco\ retained} = C_{FAaco}(V_{SAaco} - V_0) \qquad (g)$$

- Aconitic acid recovery rate, R_{Aaco}, which represents the quantity of aconitic acid recovered until a given elution fraction n ($\sum_0^n m_{Aaco}$), as compared with the maximal quantity that can be recovered in the elution peak:

$$R_{Aaco} = 100 \frac{\sum_0^n m_{Aaco}}{m_{Aaco\ tot\ recovered}} \qquad (\%) \qquad (10)$$

- Aconitic acid apparent purity, P_{app}, which compares the mass of aconitic acid in solution with the mass of the global anionic species analyzed simultaneously (including Aaco, Cl, Sul, Alac, Aace and Acit). During elution, it is calculated from the beginning to the n-th fractions considered :

$$P_{app} = 100 \frac{\sum_0^n m_{Aaco}}{\sum_0^n m_{Anions}} \qquad (\%) \qquad (11)$$

This purity criterion is used instead of *P* to estimate the purity evolution during the elution step especially, as dry matter measurement on each collected fraction would have been very cumbersome.

2.4.3. Governing equations of the separation modeling tool

A model based on classical mass conservation equations was written for ion-exchange in fixed-bed with 3 ions of equal valence. For the mobile phase, convective flow with axial dispersion was considered. For each of the species, the hypothesis of a local and instantaneous equilibrium between liquid and resin phases was assumed.

The mass conservation for solute i in the mobile phase written for each position z along the length of the column (0 < z < L) takes the form:

$$\frac{\partial x_i}{\partial t} + \frac{q_{tot}}{\varepsilon N}\frac{\partial y_i}{\partial t} + \frac{u}{\varepsilon}\frac{\partial x_i}{\partial z} = D_{ax}\frac{\partial^2 x_i}{\partial z^2} \quad (12)$$

With

x_i = ionic fraction of solute i in solution, assumed uniform on a section of the column

ε = Resin bed porosity (-)

D_{ax} = axial dispersion coefficient in the column ($m^2\ s^{-1}$)

L = column length (m)

u = linear velocity of the fluid assumed uniform on a section of the column ($m\ s^{-1}$)

For a mixture of 3 components, the time derivatives of the ionic fraction of i in the resin can be calculated from the time derivatives of the ionic fraction of i in the solution noting that:

$$\left(\frac{\partial y_2}{\partial t}\right)_{x_2,x_3,z} = \left(\frac{\partial y_2}{\partial x_2}\right)_{x_3}\left(\frac{\partial x_2}{\partial t}\right)_z + \left(\frac{\partial y_2}{\partial x_3}\right)_{x_2}\left(\frac{\partial x_3}{\partial t}\right)_z$$

And

$$\left(\frac{\partial y_3}{\partial t}\right)_{x_2,x_3,z} = \left(\frac{\partial y_3}{\partial x_2}\right)_{x_3}\left(\frac{\partial x_2}{\partial t}\right)_z + \left(\frac{\partial y_3}{\partial x_3}\right)_{x_2}\left(\frac{\partial x_3}{\partial t}\right)_z \quad (13)$$

Furthermore, it is assumed that ion exchange equilibrium for solute i in a mixture of n solutes is affected by other solutes through a competition law according to:

$$y_i = \frac{K_{x\,\mathrm{i/j}}\, x_i}{\sum_{i=1}^{n} K_{x\,\mathrm{i/j}}\, x_i} \qquad (14)$$

leading for example for j = 1 and i = 2 and 3 respectively, to :

$$y_2 = \frac{K_{x2/1}\, x_2}{1+(K_{x\,2/1}-1)x_{\,2}+(K_{x\,3/1}-1)x_{\,3}} \; ; \; y_3 = \frac{K_{x3/1}\, x_3}{1+(K_{x\,2/1}-1)x_{\,2}+(K_{x\,3/1}-1)x_{\,3}} \text{ and } y_1 = 1 - y_2 - y_3$$

Initial and boundary conditions:

- At $t = 0$ whatever z, (x_{Aaco}, y_{Aaco}) = 0 and (x_{Cl}, y_{Cl}) or (x_{Sul}, y_{Sul}) = 1, depending on the resin initial form (either chloride or sulfate)
- At $z = 0$ and $t > 0$, $$\left(\frac{\partial x_i}{\partial z}\right)_0 = \frac{u}{\varepsilon\, D_{ax}}\left(x_{i,0} - x_{Fi}\right) \qquad (15)$$

with x_{Fi} = ionic fractions of Aaco, Cl or Sul in the feed, calculated according to the analyzed composition of the synthetic solution or the standard stillage tested, and taking account of their valence for the given pH.

- At $z = L$, $$\left(\frac{\partial x_i}{\partial z}\right)_L = 0 \qquad (16)$$

A spatial discretization of these equations led to a system of ordinary differential equations. This system was solved using a dedicated algorithm “ode15s” developed in Matlab® computing software (The Mathworks Inc., Natick, Mass, USA) and adapted to stiff systems where each of unknown variables may exhibit radically different variation kinetics. This algorithm automatically adjusts the time step used for numerical integration of the equations. It allowed the ionic species breakthrough curves ($x_i = \mathrm{f}(t)$) and further $C_i = \mathrm{f}(t)$ to be calculated at the outlet of the column (at $z = L$).

2.5. Homopolar electrodialysis experiments

In the purpose of decreasing the competing anions (chlorides or sulfates) of the stillage before ion-exchange and possibly increase resin capacity and separation performances, electrodialysis was introduced as a preliminary step. Experiments were performed with a conventional two-compartment electrodialyzer TS-2-10 from EURODIA (Pertuis, France), containing seven pairs of anion- and cation-exchange membranes alternately arranged for a total effective area of 0.14 m². Anion-exchange NEOSEPTA AMX and cation-exchange NEOSEPTA CMX membranes from Tokuyama Soda (Japan) were used. Experiments were run at room temperature in batch recycling mode with two tanks (diluate and concentrate) containing 2 L solution each. Stillage (in the diluate tank) and 5 g L^{-1} NaCl solution (in the concentrate tank) were both pumped at 200 L h^{-1} in the system and recirculated. A Na_2SO_4 solution (12 g L^{-1}) was circulated through the electrode compartments to ensure electric power conduction. A constant tension of 18 V was found suitable for operating the system. During all trials, pH and conductivity were monitored in the concentrate and the diluate compartments, and current intensity was monitored. Samples were taken throughout the experiments for HPIC analyses.

- Retention rate for solute i during the ED process is defined as:

$$\text{Retention rate} = 100\left(\frac{[\text{i}](\text{g L}^{-1}) \text{ in the diluate at time t}}{[\text{i}](\text{g L}^{-1}) \text{ in the diluate initially}}\right) \quad (\%) \qquad (17)$$

- A demineralization rate was defined relatively to chloride or sulfate removal as:

$$\text{Demineralization rate} = 100\left(1 - \frac{[\text{Cl or Sul}](\text{g L}^{-1}) \text{ in the diluate after electrodialysis}}{[\text{Cl or Sul}](\text{g L}^{-1}) \text{in the initial stillage}}\right) (\%) \quad (18)$$

3. Results and discussion

3.1. Ion exchange characterization

Depending on the pH, aconitic acid exists either in non-ionized or ionized forms ($H_3Aaco/H_2Aaco^-/HAaco^{2-}/Aaco^{3-}$ - Figure 2) expected to behave differently in the ion-exchange process. Usually, the higher the aconitate valence, the higher the resin affinity for this form[34]. But this could be at the expense of the mass capacity of the resin for this acid. Actually, if one aconitate molecule interacts through several anionic groups rather than one, it might occupy more cationic sites on the resin, resulting in a decreased adsorption capacity. For monovalent aconitate (H_2Aaco^-), ion exchange isotherm results were obtained for equilibrium pH values inferior to 3.3 (Figure 3.a.), where it represents between 94 – 99 % (in eq L^{-1}) of its global ionized forms. K_x values estimated from Eq. 2 and 4 are:

K_x H_2Aaco^-/Cl^- = 5.7 and K_x H_2Aaco^-/SO_4^{2-} = 0.07 (for 0.001 < N < 0.007 eq L^{-1}).

From these, value of K_x SO_4^{2-}/Cl^- = 464 can be deduced.

It should be noted that in the case of aconitate/sulfate mixtures and for this pH range, monovalent sulfate (HSO_4^-) represents between 4.5% and 9% of its global ionic charge. Preference for SO_4^{2-} is therefore somewhat underestimated.

For four experiments with sulfate, equilibrium pH was in the range 4 – 5.6, close to the natural pH of the stillage, for which divalent aconitate form ($HAaco^{2-}$) is also present. Due to the very few number of experimental points it is hardly possible to optimize together K_x H_2Aaco^-/SO_4^{2-} and K_x $HAaco^{2-}/SO_4^{2-}$ parameters in that case. However, results clearly show a stronger affinity for aconitate than for SO_4^{2-} (Figure 3.b.). Behavior of the divalent species was considered as prevalent in that case and Eq. 2 applied to appreciate the ion exchange coefficient between both aconitate forms together (then noted

Aaco) and SO_4^{2-}. A much higher coefficient than for monovalent aconitate alone was found: K_x Aaco/SO_4^{2-} ≈ 5.

As expected[34], K_x values and curves shape reflect a strong preference of this weak anionic resin for the divalent species, $HAaco^{2-}$ being preferred to SO_4^{2-}, followed by monovalent aconitate and eventually chloride ions.

Overall isotherm results allowed the total ion exchange capacity q_{tot} of the resin to be estimated. Whatever the ion pairs and the pH, it reached a constant value of 3.4 ± 0.5 meq g_R^{-1}, showing that all the solutes under concern interact in direct relation to their valence. Given the density of the resin in the free-base form (measured here at 324 g_R L_R^{-1} (FB)), it corresponds to q_{tot} = 1.1 eq L_R^{-1}, much less than the specification of the supplier (1.7 eq L_R^{-1} (FB)). Titration of the resin successively by HCl and NaOH allowed a total capacity of about 5 meq g_R^{-1} (or 1.6 eq L_R^{-1}) to be calculated, confirming that when only minerals are concerned, capacity value obtained is close to the supplier's specification. The high molar mass of aconitic acid may cause steric hindrance for the access to all ion exchange sites, and especially inside the resin bead.

3.2. Aconitic acid purification by anion-exchange

3.2.1. Separation during the saturation phase

Both chloride and sulfate forms of the LEWATIT ® S4528 resin were tested. An experiment with a solution of aconitic acid alone adjusted at pH 4.5 on LEWATIT® S4528 column in sulfate form was run to appreciate the maximal capacity that could be reached for this solute. From the breakthrough curve analysis, it was found $V_{s\ Aaco}$ = 16.7 BV (Eq. 6), corresponding to $q_{max\ Aaco}$ = 94 g L_R^{-1} (Eq. 7) (Table 4). Expressed in ionic capacity, it represents a q_{tot} value of 1 eq L_R^{-1} (FB) consistent with previous results in batch mode.

For the same resin form fed with the standard stillage (at natural pH 4.5) (Figure 4), V_{sAaco} drops to about 12.5 BV, and the corresponding resin capacity for aconitic acid to 57 g L_R^{-1} (± 7 g L_R^{-1}) (or 0.238 g g_R^{-1}; for $C_{F\,Aaco}$ = 4.97 g L^{-1}). As expected, aconitate is preferred to monovalent organic acids and to minerals contained in the stillage: acetic and lactic acids are not retained (V_s close to V_0), probably because of their lower valence; sulfate ions initially present in the conditioned resin are displaced, due to competition effects (x_{Sul} decreases from 1 to 0.2). Even if the tricarboxylic citric acid may compete for ion exchange, it is quite not retained due to its much lower concentration: 1.3 mmol L^{-1} against 29 mmol L^{-1} for aconitic acid. Chloride ions then appear as the major competing species for this resin form, with retention of 11.2 g L_R^{-1} (for $C_{F\,Cl}$ = 4.2 g L^{-1}).

For the chloride form of the resin and the same standard stillage (not shown here), similar behavior is observed, but with a switch between chloride and sulfate. Aconitic acid breakthrough is about $V_{s\,Aaco}$ = 10 BV, corresponding to a capacity of 49 g L_R^{-1} (± 6 g L_R^{-1}) (or 0.204 g g_R^{-1}, for $C_{F\,Aaco}$ = 5.3 g L^{-1}), in the same order of magnitude than previously. Capacity for competing sulfate is there 10 g L_R^{-1} (for $C_{F\,Sul}$ = 3.0 g L^{-1}).

In order to optimize the chromatographic step and take the variability of stillage composition into account, behavior of a synthetic solution containing only aconitic acid, chloride and sulfate was studied. Both chloride and sulfate forms of the resin were tested, as well as two pH values: pH 4.5, the natural pH of the stillage; pH 3.6, where monovalent aconitate predominates. The modeling tool of ion-exchange in column was used to adjust hydraulic (D_{ax}) and selectivity coefficients ($K_{xi/j}$) by comparison between calculated and experimental breakthrough curves (best fit results). As the model accounts for equilibrium between homovalent species, all solutes "families" were initially considered as carrying a same monovalent charge. The set of coefficients noted then K_x Aaco/Cl, K_x Aaco/Sul and K_x Sul/Cl together with the hydraulic D_{ax} parameter were adjusted on the

breakthrough results of two experiments run with the synthetic solution at pH 4.5, on the resin respectively in sulfate and chloride forms (Figure 5). A $D_{ax} = 10^{-5}$ m² s^{-1} value was then found and kept once for all for further simulations.

As shown in Figure 5.a. for pH 4.5 and resin in sulfate form, breakthrough curves of the 3 components are well represented by the coefficients pair K_x Aaco/Cl = 5.3 and K_x Aaco/Sul = 3.2 (then K_x Sul/Cl = 1.66). Plateau height discrepancy between experimental points and simulations can be related to analytical errors. Ion exchange coefficient between aconitate and chloride (K_x Aaco/Cl = 5.3) is very close to K_x H_2Aaco^- / Cl^- = 5.7, obtained during batch isotherm experiments at pH ≈ 3 (Table 5), suggesting that in competition with chloride, resin affinity for aconitate is always higher and constant whatever its ionized state, mono or divalent. Concerning the exchange between aconitate and sulfate, coefficients obtained through column and batch experiments at pH = 4.5 are in the same order of magnitude (respectively K_x Aaco/Sul = 3.2 and K_x Aaco/ SO_4^{2-} ≈ 5). For the record, these species are considered as carrying the same charge for both models. These adjusted coefficients also well account for the behavior of the 3 components when the resin is initially conditioned in chloride form (Figure 5.b.).

Aconitic acid retention for the synthetic solution at pH 4.5 is equivalent for both conditionings, at about 70 g L_R^{-1} (Table 4), a capacity higher by about 30% to that for the standard stillage. This can be explained by the presence of the additional solutes in this latter. As already mentioned, aconitic acid purity is $P \approx 6$ % (w/w) in the standard stillage, which also contains 12% of -chloride plus sulfate- and quite the same for the additional organic acids (neglected in the simulation). Non-analyzed compounds, including coloring matters, then represent about 70 % (w/w) of the stillage (or a concentration of about 70 g L^{-1} for DM in the stillage at about 10%). In the synthetic solution, aconitic acid purity is

much higher at $P \approx 32$ % (w/w), chloride and sulfate representing the remaining part (68 %). The impact of the neglected additional solutes to ion-exchange and aconitic acid retention appears finally quite limited in regards to their contribution to the stillage dry matter (82%), which confirms the relevancy of this approach based on the behavior of a synthetic solution.

As a result, the coefficients set applied to simulate standard stillage saturation on both resin forms leads to a correct description of the breakthrough shapes, but to an over-estimation of the capacity for aconitate (example in Figure 6 for resin under chloride form).

The influence of pH on resin selectivity and capacity for aconitic acid was also investigated. As observed for the isotherms, increasing the aconitate valence leads to a higher affinity with the resin; but it could also cause a decrease in mass (or molar) capacity, as a divalent form occupies two resin sites instead of one for a monovalent form. Example for the resin in sulfate form is given for both synthetic solution and standard stillage in Figure 7. For breakthrough simulation, K_x Sul/Cl was considered as non-affected by pH change (K_x Sul/Cl = 1.66). Only the rational selectivity coefficient between aconitate and sulfate was adjusted for the synthetic solution results (Figure 7.a.), with K_x Aaco/Sul = 1.8, much lower than at pH 4.5, due to the predominance of aconitate monovalent form (K_x Aaco/Cl = 3 then arises). Thanks to this modification, the breakthrough of Aaco, Sul and Cl is correctly predicted, for the synthetic solution as well as for the standard stillage (Figure 7.b.).

All in all, working at pH 3.6 led to a decrease of aconitic acid mass capacity of 12% and 20% for synthetic solution and standard stillage, respectively (Table 4). For further

studies, pH = 4.5 was then considered as the best choice for aconitic acid separation from sugarcane stillage.

3.2.2. Elution performances

Elution was studied after loading steps with standard stillage at pH 4.5 on the resin in sulfate and chloride forms. Elution curves are given in Figure 8. A regeneration yield Y_{Aaco} in aconitic acid of about 72 % was achieved in both cases. Being non-ionized at the acidic pH of the elution solution, aconitic acid elutes first (from 2 BV) and the apparent purity P_{app} of the cumulated fractions reaches a maximum of $P_{app\ max} \approx 90$ % at about 3 BV. It was about 23 % initially in the standard stillage. It further decreases with the breakthrough of minerals. Recovery rate and apparent purity developing in opposite directions after that, elution fractions were considered pure enough until about 4.2 BV, which corresponds to a recovery rate of $R_{Aaco} = 82$ % for resin under sulfate form and elution with sulfuric acid 0.5 N (Figure 8.a.) and 85 % for resin under chloride form and elution with hydrochloric acid 0.5 N (Figure 8.b.). Purity evaluation of the fractions of interest (in the range 2 BV to ≈ 4.2 BV) was respectively $P_{app} = 83$ % and 80 %. At the same time P increases from 6 % initially to 32 % (w/w) for both (Table 6), which corresponds to a purification factor of x 3.3 regarding P_{app} and over x 5 regarding P. Dry matter is also composed of about 10 % of both minerals, and 1.5 % of additional organic acids; non analyzed compounds then still represent about 56 % of the DM of these fractions.

This chromatographic step has contributed not only to the elimination of about 90 % of the competing organic acids but also to that of about 40 % of the unquantified components in the stillage. At the same time aconitic acid has been threefold concentrated.

Even if ion exchange appears efficient in extracting aconitic acid from sugar cane stillage, elution fractions collected still contain chloride and sulfate ions (at concentrations lower from 3 to 10 times respectively as compared with the feed) and are still colored. Moreover, the ion-exchange experiment with aconitic acid alone showed that a resin capacity increase of 65% for this acid was achievable, provided the removal of minerals. This would increase the effectiveness of the ion-exchange step and at the same time improve the quality of the eluted fractions.

3.2.3. Study of the impact of a demineralization step on the anion-exchange performances

The ion exchange parameters set obtained previously was used to predict the aconitic acid breakthrough for decreased concentrations of minerals (chloride for the sulfate form of the resin, and sulfate for the chloride form), as could be obtained after a preliminary demineralization step. As expected, for resin in sulfate form, a decrease of the chloride content of a synthetic solution results in shifting the aconitic acid breakthrough towards higher V_s with a maximal predicted capacity around 94 g L_R^{-1} (Figure 9), consistent with the result for aconitic acid alone (Table 4). Calculating capacities for aconitic acid versus the corresponding demineralization rate (Figure 10) clearly indicates that sulfate removal is less interesting than chloride one, as only 77 g L_R^{-1} for aconitic acid is then achieved. This can be explained by the fact that the initial sulfate concentration in the stillage studied is much lower than is chloride, with x_{Sul} = 0.2, when x_{Cl} = 0.6. Even after a complete sulfate removal and if chloride are not affected by this pretreatment, chloride would still represent 75 % of the global ionic charge of the solution. Moreover, both figures show that there is little interest in decreasing chloride content below 0.5 g L^{-1} (or x_{Cl} below 0.14) which corresponds to a demineralization rate of 89%.

Conventional electrodialysis was then used as pre-treatment step to decrease chloride content.

3.3. Treatment of the standard stillage by combination of electrodialysis and anion-exchange steps

Electrodialysis studied with the standard stillage (pH 4.5) shows that after 10 min, aconitate retention rate in the diluate decreases, as transfer towards concentrate begins (Figure 11). However its loss towards the concentrate after 15 minutes is only about 5% when simultaneously, chloride one is 95%. As expected [16, 32, 33] electrodialysis is efficient to eliminate chloride ions of the stillage, at the expense of a moderate loss of aconitate. Simultaneously, sulfate ions stay with aconitate ions at more than 90% in the diluate, even after 25 minutes (Table 7). Citrate also remains in the diluate, probably due to its high charge and hydration: it appears sterically hindered and behaves as aconitate. For combination of electrodialysis pretreatment and ion-exchange purification, electrodialysis was performed during 25 min in order to reach the lowest chloride concentration of 0.2 g L^{-1}, which corresponds to a demineralization rate of about 96%. As previously mentioned, it could have been stopped sooner as no real benefit shall be observed on ion-exchange performances for a chloride content below 0.5 g L^{-1}. After this step, aconitic acid purity was measured quite unchanged at $P \approx 6$ % while its apparent purity was increased by a factor x 1.5, from $P_{app} \approx 23\%$ until 35%.

The demineralized stillage was further purified by anion-exchange on the LEWATIT® S4528 resin under sulfate form. Breakthrough curves are given in Figure 12. As expected, capacity for aconitic acid was increased from 57 g L_R^{-1} (standard stillage) up to 78 g L_R^{-1} ($V_{s\,Aaco}$ = 16.4 BV). Actually, the demineralization step results in an increase of x_{Aaco} from about 0.2 until 0.51. Even if aconitic acid breakthrough seems close to that when it is alone in the same pH condition, the corresponding capacity of about 94 g L_R^{-1} is not

reached, due to the sulfates still present in the feed (x_{Sul} = 0.44), or to other compounds neglected until then and not quantified as already discussed.

Chloride removal by conventional electrodialysis finally allowed the duration of the chromatographic loading step to be enhanced by 30%. Further elution by H_2SO_4 0.5 N led to a very acidic extract (pH ≈ 1) (eluted fractions from 2.1 to 4.4 BV) containing aconitic acid at P_{app} = 86 % and P = 39 % (Table 8). Other analyzed anions contributed to 6% (w/w) instead of 24% initially in the standard stillage. Non-analyzed compounds still represent more than 50% of the dry matter and the fractions are still colored.

4. Conclusions

Sugarcane stillage in the Reunion Island (French overseas department) could be better valorized by extraction of interesting organic solutes including aconitic acid. Separation of this tricarboxylic acid from other organic acids and minerals was studied by anion-exchange on LEWATIT® S4528 resin (weak base resin). Ion-exchange experiments in batch mode showed a strongest affinity for the divalent form of the aconitate, followed by sulfate, monovalent aconitate and at last chloride. From the analysis of the total capacity of the resin obtained for different combinations of the different ions, it also emerged that the divalent form of the aconitate interacts with the ionic sites of the resin through its two charges. Fractionation in column was then studied on sulfate and chloride forms of the resin, and for two pH values in order to compare the selectivity and mass capacity for monovalent form (majority at pH 3.6) and a mixture of monovalent and divalent forms of the aconitate (for natural pH 4.5 of the stillage). For a given resin bed volume, mass capacity appeared to be the highest in the case of the natural stillage pH (4.5), and that whatever the resin form, showing that the charge effect remains beneficial. A modelling tool describing the fractionation of homovalent species during ion-exchange

in column was elaborated to investigate the behavior of the solutes for the different pH, resin forms, and solutes proportions in the stillage. After adjustment of the ion-exchange parameters using a synthetic stillage, the impact of a pre-demineralization step on the resin capacity for aconitic acid could be evaluated. Elimination of chloride until 0.5 g L^{-1} appeared as the best option. Electrodialysis was then run to eliminate quite completely chloride ions in the concentrate with a very limited loss of the acid. In a certain extent, it also led to a decrease in lactate and acetate ions contents. Separation of the remaining organic acids in the demineralized stillage, especially monovalent ones, was run through the anion-exchange step, with resin in sulfate form. Previous elimination of chloride from the stillage allowed to reach 82.5% of the maximum retention capacity of this acid, when it was only 62% for the standard stillage. Elution with H_2SO_4 0.5 N led to a purification factor for aconitic acid of about 7 relatively to *P* (%DM)), a concentration factor about x 3, for a global yield about 40% (Figure 13). Through these steps, the proportion of other analyzed anions in the dry matter decreased from 24% to 6%, when for non-analyzed solutes (including coloring) it was from 70% to 56%.

It appears clearly that complementary steps should now be added and studied, upstream or downstream of ion-exchange. Especially, study of discoloration on an adsorbent resin of the stillage and of the eluate after ion-exchange has already been undertaken [35]. The latter gives very positive results, with up to 90% of color elimination together with a limited loss in aconitic acid, which might enable a direct crystallization afterwards.

Acknowlegments

Authors wish to thank Tereos, eRcane for their financial and technical support especially for HPIC analyses.

References

[1] Caderby, E.; Baumberger, S.; Hoareau, W.; Fargues, C.; Decloux, M.; Maillard, M. N. (2013). Sugar Cane Stillage: A Potential Source of Natural Antioxidants. *Journal of Agricultural and Food Chemistry,* 61(47): 11494.

[2] Zapata, N. J. G. (2007). *Aconitic acid from sugarcane: production and industrial application.* Louisiana State University, USA, Baton Rouge.

[3] Blinco, J. A. L.; Doherty, W. O. S. (2005). Review of extraction technologies for organic acid production. In *27th Australian Society of Sugarcane Technology Conference*). Queensland, Australia.

[4] de Oliveira, D. P.; Augusto, G. G.; Batista, N. V.; de Oliveira, V. L. S.; Ferreira, D. S.; Souza, M.; Fernandes, C.; Amaral, F. A.; Teixeira, M. M.; de Padua, R. M.; Oliveira, M. C.; Braga, F. C. (2018). Encapsulation of trans-aconitic acid in mucoadhesive microspheres prolongs the anti-inflammatory effect in LPS-induced acute arthritis. *European Journal of Pharmaceutical Sciences,* 119: 112.

[5] Fang, X. B.; Zhang, J. M.; Xie, X.; Liu, D.; He, C. W.; Wan, J. B.; Chen, M. W. (2016). pH-sensitive micelles based on acid-labile pluronic F68-curcumin conjugates for improved tumor intracellular drug delivery. *International Journal of Pharmaceutics,* 502(1-2): 28.

[6] Voll, E.; Gazziero, D. L. P.; Adegas, F. S. (2010). Aconitic Acid on Seeds of Weed Species from Different Locations. *Planta Daninha,* 28(1): 13.

[7] Kanitkar, A.; Smoak, M.; Chen, C.; Aita, G.; Scherr, T.; Madsen, L.; Hayes, D. (2016). Synthesis of novel polyesters for potential applications in skin tissue engineering. *Journal of Chemical Technology and Biotechnology,* 91(3): 733.

[8] Saeed, H. A. M.; Eltahir, Y. A.; Xia, Y. M.; Wang, Y. M. (2014). Synthesis and characterization of aliphatic-aromatic hyperbranched polyesters with high organosolubility. *Russian Journal of Applied Chemistry,* 87(10): 1481.

[9] Joo, Y. C.; You, S. K.; Shin, S. K.; Ko, Y. J.; Jung, K. H.; Sim, S. A.; Han, S. O. (2017). Bio-Based Production of Dimethyl Itaconate From Rice Wine Waste-Derived Itaconic Acid. *Biotechnology Journal,* 12(11): 1.

[10] Xie, X. N.; Xu, S. P.; Pi, P. H.; Cheng, J.; Wen, X. F.; Liu, X.; Wang, S. N. (2018). Dissipative Particle Dynamic Simulation on the Assembly and Release of siRNA/Polymer/Gold Nanoparticles Based Polyplex. *AIChE Journal,* 64(3): 810.

[11] Werpy, T.; Petersen, G. (2004). Top Value Added Chemicals from Biomass - Volume I—Results of screening for potential candidates from sugars and synthesis gas. In, (pp. 76). SW Washington, U.S.: U.S. Department of Energy.

[12] Cranston, H. A. (1951). Manufacture of aconitic acid. In, vol. US 2,566,172 (pp. 1). USA: Daniel F Kelly.

[13] Collier, D. W. (1950). Process of treating aconitic acid containing plant extracts. In S. Corp (Ed.), vol. US 2,513,287 (pp. 1). USA: Sharples Corp.

[14] Kanitkar, A.; Aita, G.; Madsen, L. (2013). The recovery of polymerization grade aconitic acid from sugarcane molasses. *Journal of Chemical Technology and Biotechnology,* 88(12): 2188.

[15] Malmary, G.; Albet, J.; Putranto, A.; Hanine, H.; Molinier, J. (2000). Recovery of aconitic and lactic acids from simulated aqueous effluents of the sugar-cane industry through liquid-liquid extraction. *Journal of Chemical Technology and Biotechnology,* 75(12): 1169.

[16] Dupoiron, S.; Lameloise, M. L.; Bedu, M.; Lewandowski, R.; Fargues, C.; Allais, F.; Teixeira, A. R. S.; Rakotoarivonina, H.; Remond, C. (2018). Recovering ferulic acid from wheat bran enzymatic hydrolysate by a novel and non-thermal process associating weak anion-exchange and electrodialysis. *Separation and Purification Technology,* 200: 75.

[17] Kuang, P. Q.; Liang, H.; Yuan, Q. P. (2010). Isolation and Purification of Glucoraphenin from Radish Seeds by Low-Pressure Column Chromatography and Nanofiltration. *Separation Science and Technology,* 46(1): 179.

[18] Fargues, C.; Lewandowski, R.; Lameloise, M.-L. (2010). Evaluation of ion-exchange and adsorbent resins for the detoxification of beet distillery effluents. *Industrial & Engineering Chemistry Research,* 49(19): 9248.

[19] Bailly, A.; Roux-de Balmann, H.; Aimar, P.; Lutin, F.; Cheryan, M. (2001). Production processes of fermented organic acids targeted around membrane operations: design of the concentration step by conventional electrodialysis. *Journal of Membrane Science,* 191(1-2): 129.

[20] Blanc, C.-L.; Theoleyre, M.-A.; Lutin, F.; Pareau, D.; Stambouli, M. (2015). Purification of organic acids by chromatography: adsorption isotherms and impact of elution flow. *Separation and Purification Technology,* 141: 105.

[21] Joglekar, H. G.; Rahman, I.; Babu, S.; Kulkarni, B. D.; Joshi, A. (2006). Comparative assessment of downstream processing options for lactic acid. *Separation and Purification Technology,* 52(1): 1.

[22] Moldes, A. B.; Alonso, J. L.; Parajo, J. C. (2003). Recovery of lactic acid from simultaneous saccharification and fermentation media using anion exchange resins. *Bioprocess and Biosystems Engineering,* 25(6): 357.

[23] Sun, X.; Lu, H.; Wang, J. (2017). Recovery of citric acid from fermented liquid by bipolar membrane electrodialysis. *Journal of Cleaner production,* 143: 250.

[24] Lee, H. D.; Lee, M. Y.; Hwang, Y. S.; Cho, Y. H.; Kim, H. W.; Park, H. B. (2017). Separation and Purification of Lactic Acid from Fermentation Broth Using Membrane-Integrated Separation Processes. *Industrial & Engineering Chemistry Research,* 56(29): 8301.

[25] Luongo, V.; Palma, A.; Rene, E. R.; Fontana, A.; Pirozzi, F.; Esposito, G.; Lens, P. N. L. (2019). Lactic acid recovery from a model of Thermotoga neapolitana fermentation broth using ion exchange resins in batch and fixed-bed reactors. *Separation Science and Technology,* 54(6): 1008.

[26] Hanine, H.; Mourgues, J.; Conte, T.; Malmary, G.; Molinier, J. (1992). Recovery of Calcium Aconitate from Effluents from Cane Sugar Production with Ion-Exchange Resins. *Bioresource Technology,* 39(3): 221.

[27] Saska, M.; Zapata, N. G. (2006). Some observations on feasibility of recovering aconitic acid from low purity sugarcane liquors. *International Sugar Journal,* 108(1288): 203.

[28] CERF. (2009). Projet V2ARUN - Valorisation d'un coproduit de la canne à sucre : l'acide aconitique. In *Compte-rendu du comité de pilotage -CRCP4*). La Réunion, France: CERF.

[29] Petit, A.; Wut-Tiu-Yen, J.; Pislor, E.; Pontalier, P.-Y.; Albet, J.; Hoareau, W.; Corcodel, L. (2015). Procédé d'extraction de l'acide aconitique à partir de produits issus de l'industrie de la canne à sucre. In I. N. P. d. T. I. Ercane, Université de la Réunion (Ed.), vol. EP2921471A1). France.

[30] Pislor, E. (2011). *Extraction d'un acide organique à partir de co-produits issus de l'industrie de la canne à sucre.* INP Toulouse, France, Toulouse, France.

[31] Huang, C. H.; Xu, T. W.; Zhang, Y. P.; Xue, Y. H.; Chen, G. W. (2007). Application of electrodialysis to the production of organic acids: State-of-the-art and recent developments. *Journal of Membrane Science,* 288(1-2): 1.

[32] Montiel, V.; Garcia-Garcia, V.; Gonzalez-Garcia, J.; Carmona, F.; Aldaz, A. (1998). Recovery by means of electrodialysis of an aromatic amino acid from a solution with a high concentration of sulphates and phosphates. *Journal of Membrane Science,* 140(2): 243.

[33] Sata, T. (2000). Studies on anion exchange membranes having permselectivity for specific anions in electrodialysis - effect of hydrophilicity of anion exchange membranes on permselectivity of anions. *Journal of Membrane Science,* 167(1): 1.

[34] Dorfner, K. (1991). *Ion Exchangers*. Berlin - New York: Walter de Gruyter.

[35] Wu-Tiu-Yen, J. (2017). *Valorisation de la vinasse de canne à sucre: étude d'un procédé d'extraction d'un acide organique multivalent.* Paris-Saclay University, Massy, France.

Tables

Table 1. Anion average composition and variability of Rivière du Mât distillery stillage (10 lots analyzed within November 2013 and June 2015)

Solutes analyzed	**Abbreviation**	**Molar mass, M (g mol^{-1})**	**Concentration and lots range (g L^{-1})**
Lactic acid	Alac	90.08	7.9 ± 1.5
Chloride	Cl	35.5	4.7 ± 2.8
Acetic acid	Aace	60.05	2.7 ± 2.0
Sulfate	Sul	96.06	2.2 ± 0.6
Formic acid	Afor	46.03	0.3 ± 0.1
Butyric acid	Abut	88.11	0.2 ± 0.1
Isocitric acid	Aisocit	192.12	0.2 ± 0.1
Citric acid	Acit		0.1 ± 0.1
Pyruvic acid	Apyr	88.06	0.1 ± 0.1
Oxalic acid	Aoxa	90.03	0.1 ± 0.04
Phosphate	Pho	94.97	0.1 ± 0.1
Trans-aconitic acid	Trans-Aaco		3.9 ± 1.0
Cis-aconitic acid	Cis-Aaco	174.1	1.6 ± 0.6
Total Aconitic acid	Aaco		5.5 ± 1.6

Table 2. Physical properties of LEWATIT® S4528

Matrix	**Functional groups**	**Exchange capacity (eq L_R^{-1} *)**	**Moisture (% w/w)**	**Max. swelling (%** FB → Cl^-**)**	**Bead diameter (mm)**	**Density (g_R L_R^{-1})**
Styrenic MR	Tertiary amine	1.7	46-52	45	0.40-1.25	620

(*) L_R = L of resin in column, free-base (FB) form

Table 3. Average standard stillage composition

C_{Aaco} (g L^{-1})	C_{Cl} (g L^{-1})	C_{Sul} (g L^{-1})	C_{Alac} (g L^{-1})	C_{Aace} (g L^{-1})	$C_{Acit + Aisocit}$ (g L^{-1})
5	4.5	2	4	2	0.5

Table 4. Summary of aconitic acid capacity in column for the different feeds and resin forms tested

Resin form	q_{Aaco} **(g L_R^{-1}) - pH 4.5**			q_{Aaco} **(g L_R^{-1}) - pH 3.6**	
	Standard stillage	Synthetic solution	Aconitic acid alone	Standard stillage	Synthetic solution
Sulfate	57 (± 7)	68 (± 8)	94 (± 10)	46 (± 5)	60 (± 7)
Chloride	49 (± 6)	74 (± 9)	/	/	/

Table 5. Values of ion-exchange rational selectivity coefficients obtained through isotherm equilibrium measurements and column experiments

pH	Species	K_x values	
		Isotherm	Column
4.5	Aaco / SO_4^{2-}	≈ 5	3.2
	H_2Aaco^- / Cl^-	-	5.3
	Sul/ Cl	-	1.66
3.6	Aaco / Sul	-	1.8
	Aaco / Cl	-	3
	Sul/ Cl	-	1.66
2.5 – 3.3	H_2Aaco^- / SO_4^{2-}	0.07	-
	H_2Aaco^- / Cl^-	5.7	-
	SO_4^{2-}/ Cl^-	464	-

Table 6. Elution performances: quality and recovery of the fractions of interest collected

Elution solution	**Volume range (BV)**	**Concentrations (g L^{-1})**						R_{Aaco} (%)	P_{app} (%)
		Aaco	**Sul**	**Cl**	**Alac**	**Aace**	**Acit**		
H_2SO_4 0.5 N	2.1 to 4.5	15.8	1.68	2.36	0.22	0.02	0.37	82	83
HCl 0.5 N	2 to 4	13.8	0.17	2.19	0.07	0.02	0.26	85	80

Table 7. Solutes retention rates in the dilution tank during ED process.

(Standard stillage - pH = 4.5; U = 18 V; AMX and CMX NEOSEPTA membranes)

Time (min)	**Retention rate (%)**					
	Aace	**Alac**	**Aaco**	**Acit**	**Cl**	**Sul**
15	51	62	95	71	5	72
25	44	58	83	100	1	93

Table 8. Quality and recovery of the fractions of interest collected during each purification step

Purification steps	**Concentrations (g L^{-1})**						Y_{Aaco} *(%)*	P_{app} **(%)**	***P*** **(% DM)**
	Aaco	**Sul**	**Cl**	**Alac**	**Aace**	**Acit**			
Standard stillage	5.8	2.1	5.0	8.9	1.0	0.7		23	6
Dechlorinated stillage	4.9	2	0.2	9.3	1.7	0.1	85 - 95	35	6
Loading on ion-exchange column							75		
Eluted fraction by H_2SO_4 0.5 N (2.1 to 4.4 BV)	16.6	2.3	0.084	0.097	0.014	0.082	59*	86	39

(*) Product of the recovery rate (R_{Aaco}) in the eluted fraction and the regeneration yield (Y_{Aaco})

Figures

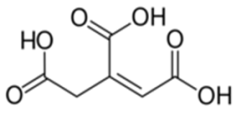

Cis-aconitic acid

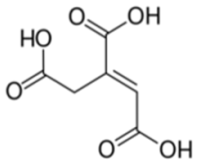

Trans-aconitic acid

Water solubility (25°C) (g/100 g solution)		33
Acidity constants (25°C)	pKa_1	2.80
	pKa_2	4.46
	pKa_3	6.30

Figure 1. Aconitic acid isomers and properties

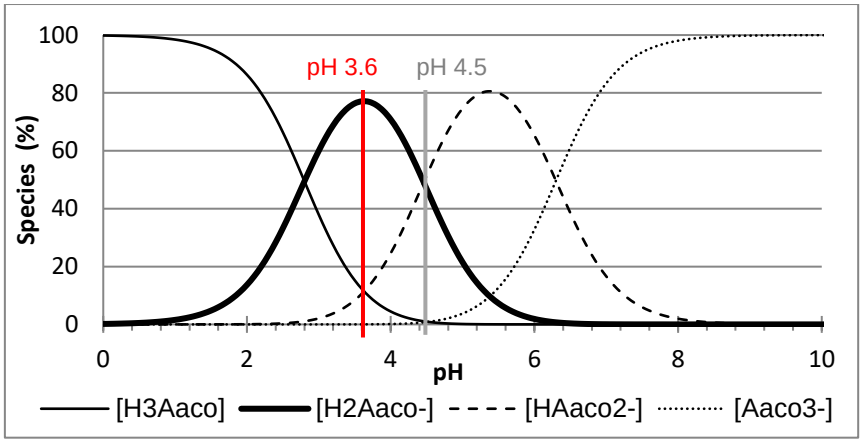

Figure 2. Aconitic acid speciation diagram

(a)

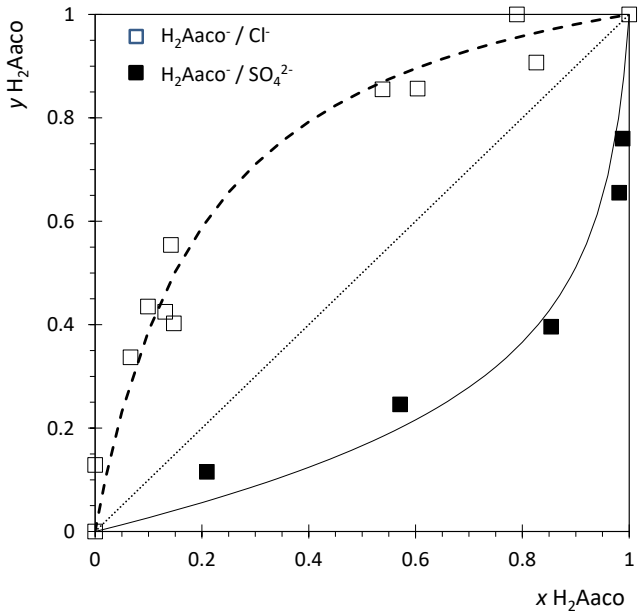

(b)

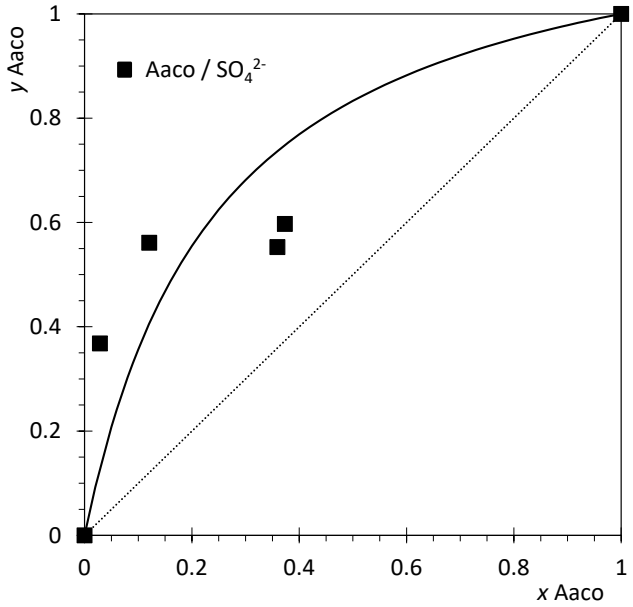

Figure 3. Ion exchange isotherms on LEWATIT® S 4528 of aconitic acid with Cl^- and SO_4^{2-}. (a) Monovalent aconitate (H_2Aaco^-) for pH = 2.5-3.3; experimental and modeling (- - - - - K_x H_2Aaco^-/Cl^- = 5.7; ——— K_x H_2Aaco^-/SO_4^{2-} = 0.07); (b) Mixture of monovalent and divalent aconitate (Aaco) for pH = 4.1 - 5.6: experimental and modeling (——— K_x $Aaco/SO_4^{2-} \approx 5$). Comparison with experimental points for monovalent aconitate only.

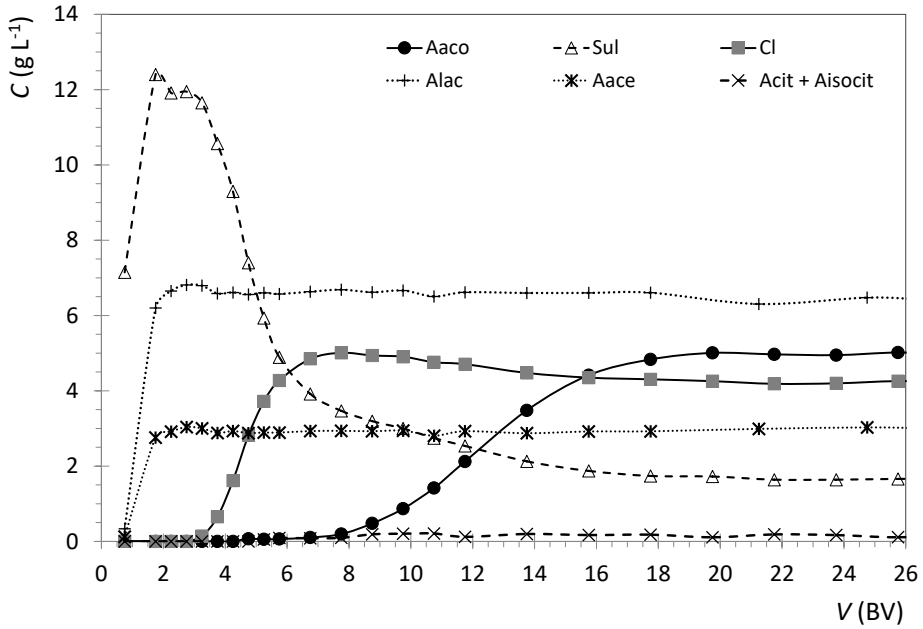

Figure 4. Breakthrough curves of main components for the standard stillage (pH 4.5) on LEWATIT® S4528 resin in sulfate form (BV = 61.9 mL).

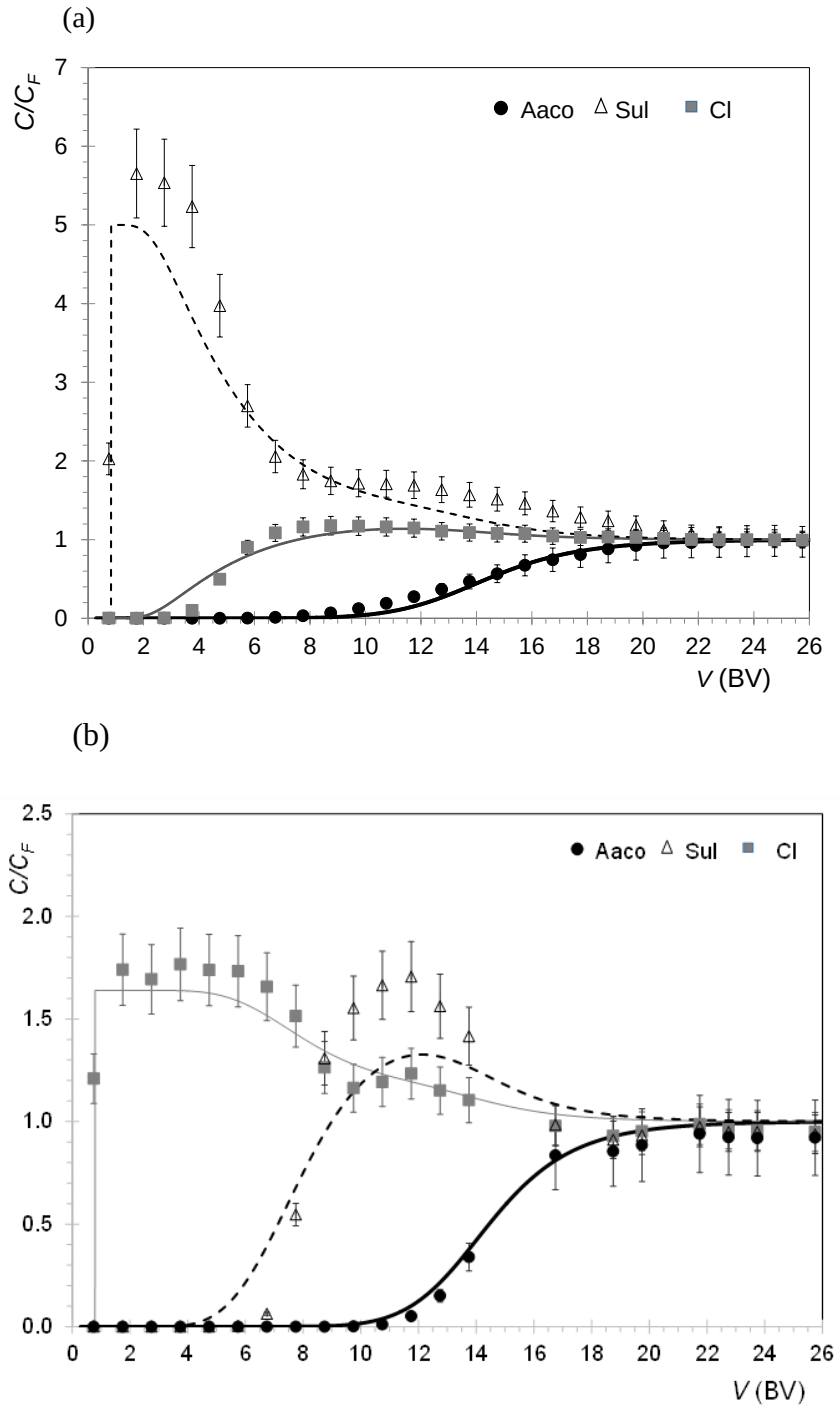

Figure 5. Experimental and simulated breakthrough curves for synthetic solution at pH 4.5 on LEWATIT® S4528 resin in (a) sulfate form; (b) chloride form.

(BV = 61 mL / 65 mL; x_{Aaco} = 0.2; x_{Sul} = 0.2; x_{Cl} = 0.6; N = 0.211 eq L^{-1}; Lines correspond to D_{ax} = 10^{-5} m^2 s^{-1}; K_x Aaco/Cl = 5.3; K_x Aaco/Sul = 3.2 (then K_x Sul/Cl = 1.66)).

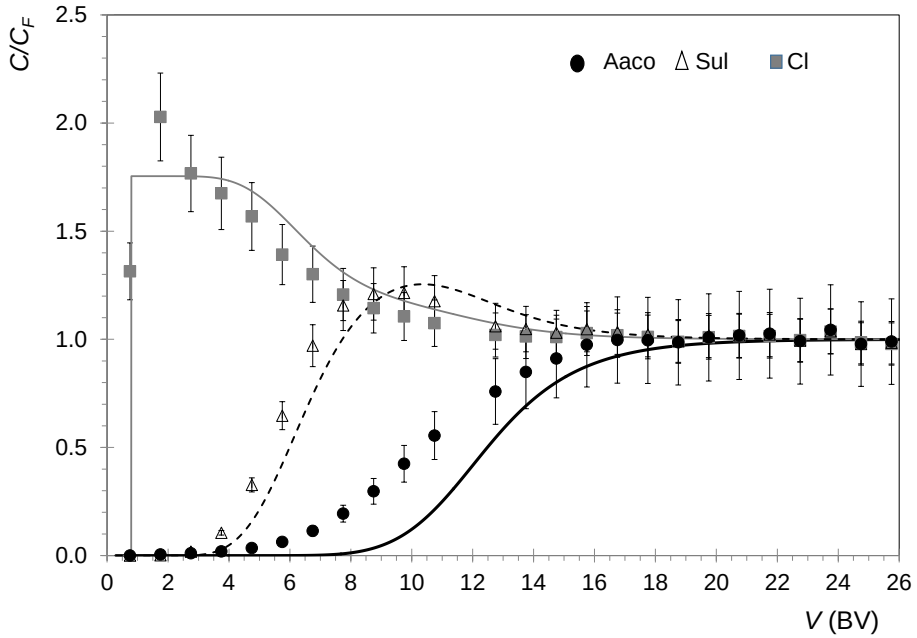

Figure 6. Experimental and simulated breakthrough curves for standard stillage at pH 4.5 on LEWATIT® S4528 resin in chloride form.

(BV = 61.5 mL; x_{Aaco} = 0.18; x_{Sul} = 0.25; x_{Cl} = 0.57; N = 0.251 eq L^{-1}- ; Lines correspond to $D_{ax} = 10^{-5}$ m^2 s^{-1}; K_x Aaco/Cl = 5.3; K_x Aaco/Sul = 3.2 (then K_x Sul/Cl = 1.66)).

(a)

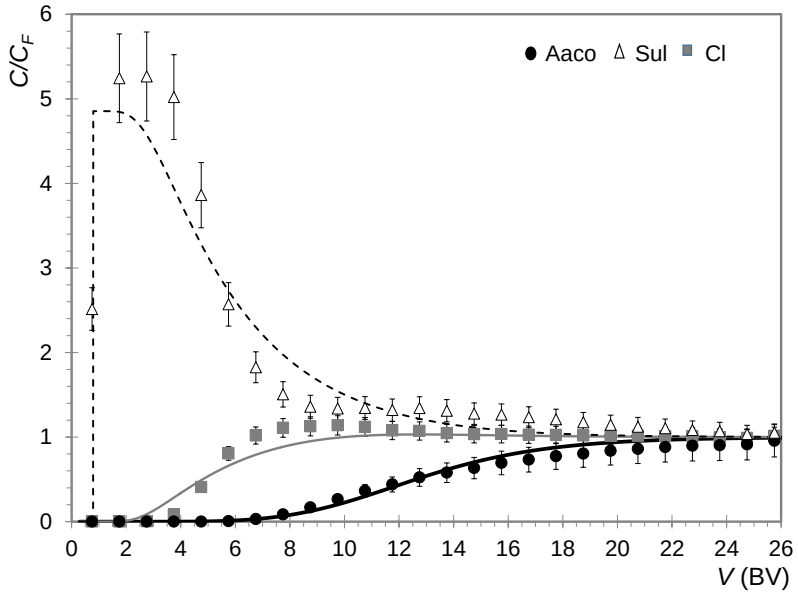

(b)

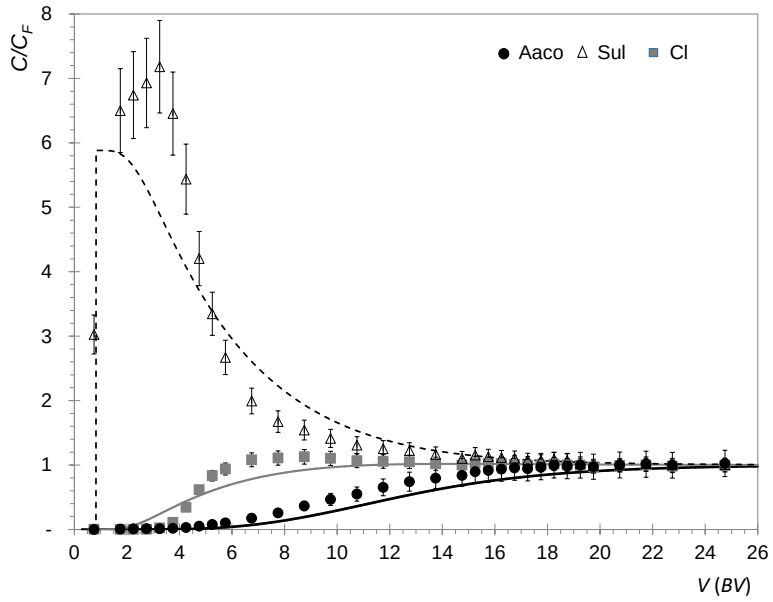

Figure 7. Experimental and simulated breakthrough curves at pH 3.6 on LEWATIT® S4528 resin in sulfate form for (a) the synthetic solution; (b) the standard stillage.

(BV = 51.4 mL / 62.2 mL; x_{Aaco} = 0.13; x_{Sul} = 0.21 / 0.17; x_{Cl} = 0.66 / 0.7; N = 0.191 eq L^{-1}/ 0.196 eq L^{-1} ; Lines correspond to $D_{ax} = 10^{-5}$ m^2 s^{-1}; K_x Aaco/Cl = 3; K_x Aaco/Sul = 1.8 (K_x Sul/Cl = 1.66 unchanged)).

(a)

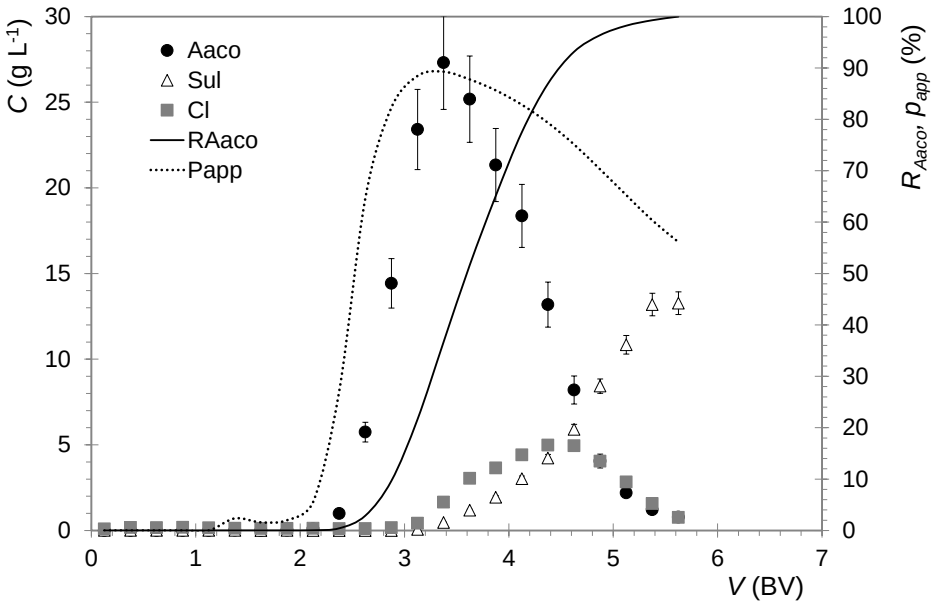

(b)

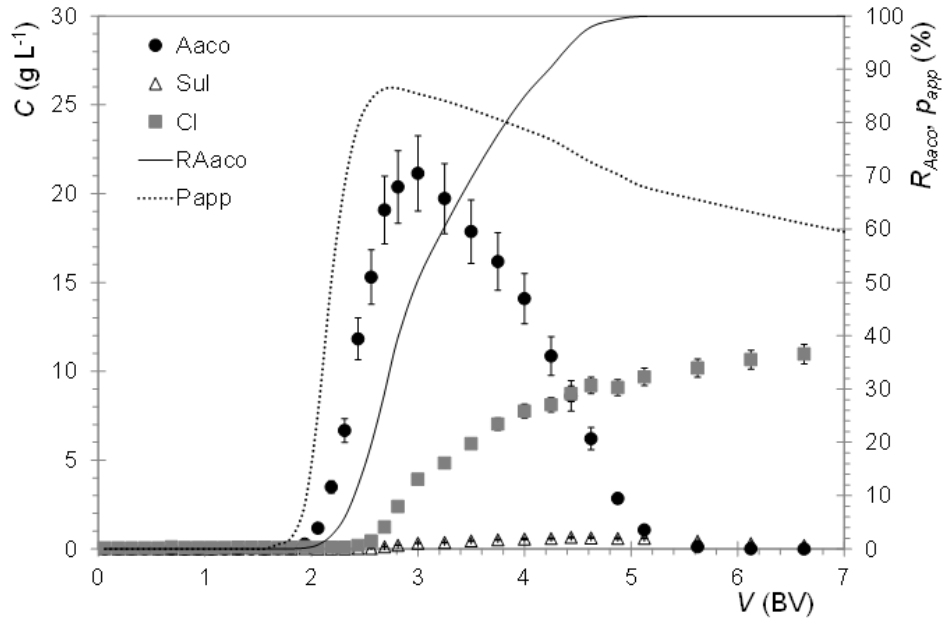

Figure 8. Elution curves of the main stillage components following a saturation step with standard stillage pH 4.5: (a) elution with H_2SO_4 0.5 N, for LEWATIT® S4528 initially under sulfate form; (b) elution with HCl 0.5 N, for LEWATIT® S4528 initially under chloride form.

(BV = 61.7 mL; elution flow-rate = 1 BV h^{-1}).

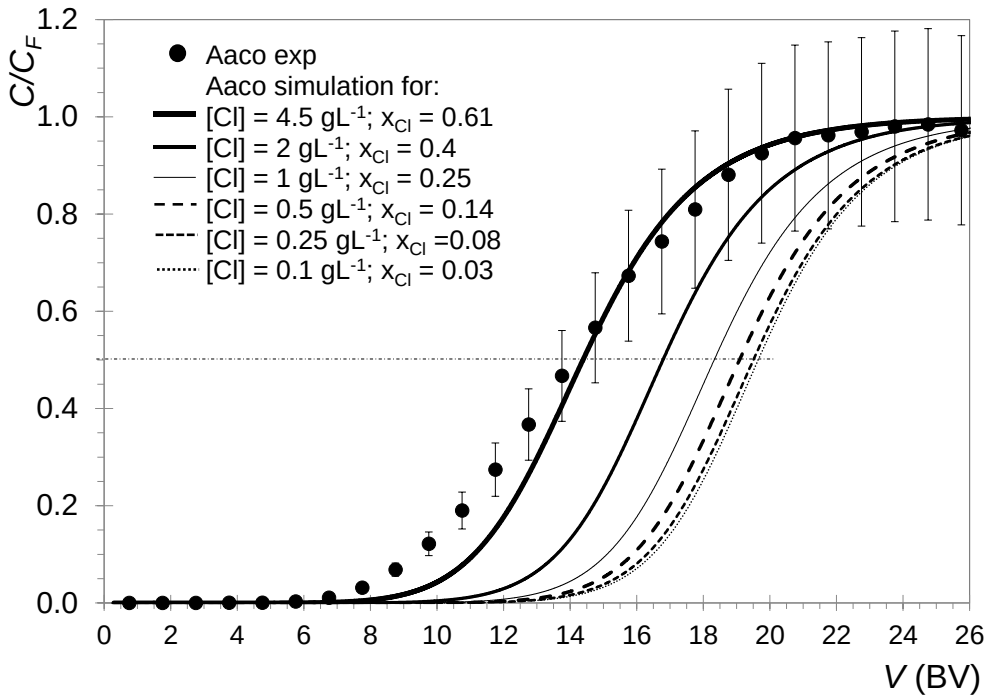

Figure 9. Simulated breakthrough of aconitic acid contained in a synthetic solution with decreasing chloride content, at pH 4.5 on LEWATIT® S4528 resin in sulfate form.

(Initial composition: $C_{Aaco\ F}$ = 5.01 g L^{-1}; $C_{Cl\ F}$ = 4.5 g L^{-1}; $C_{Sul\ F}$ = 1.91 g L^{-1} - Lines correspond to D_{ax} = 10^{-5} m^2 s^{-1}; K_x Aaco/Cl = 5.3 ; K_x Aaco/Sul = 3.2 (then K_x Sul/Cl = 1.66)).

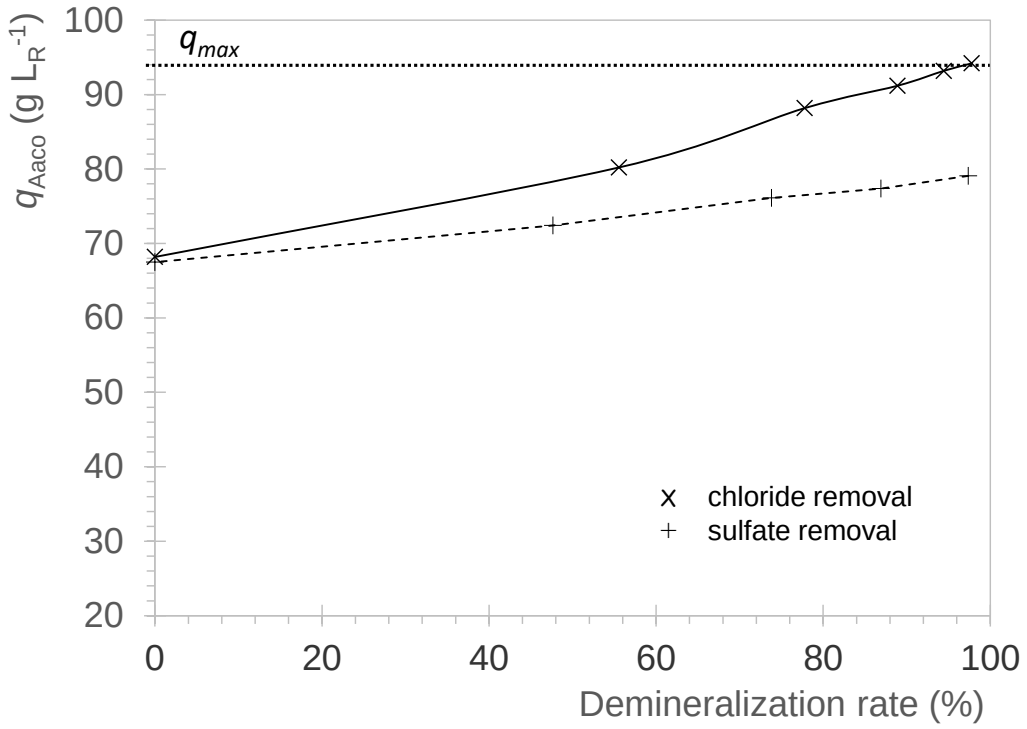

Figure 10. Simulation of the influence of the demineralization rate on the resin capacity for aconitic acid (chloride removal: resin in sulfate form; sulfate removal: resin in chloride form).

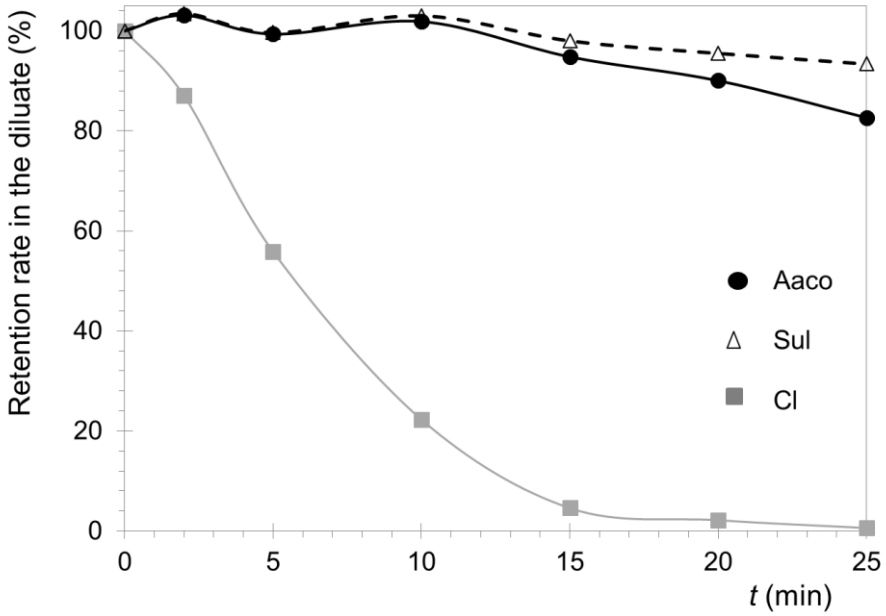

Figure 11. Evolution of the solutes retention rates in the diluate during electrodialysis (standard stillage – pH 4.5; U = 18 V; AMX and CMX NEOSEPTA membranes).

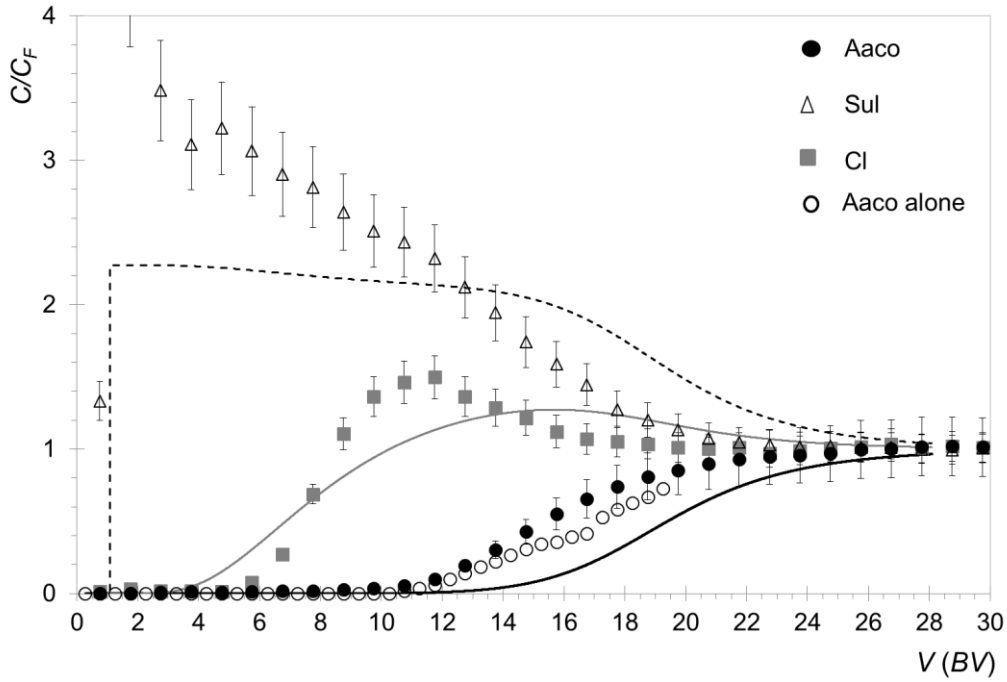

Figure 12. Experimental and simulated breakthrough curves at pH 4.5 on LEWATIT® S4528 resin in sulfate form for standard stillage after chloride removal by electrodialysis (BV = 49.8 mL; x_{Aaco} = 0.51; x_{Sul} = 0.44; x_{Cl} = 0.05; N = 0.088 eq L^{-1}; Lines correspond to $D_{ax} = 10^{-5}$ m^2 s^{-1}; K_x Aaco/Cl = 5.3 ; K_x Aaco/Sul = 3.2 (then K_x Sul/Cl = 1.66)).

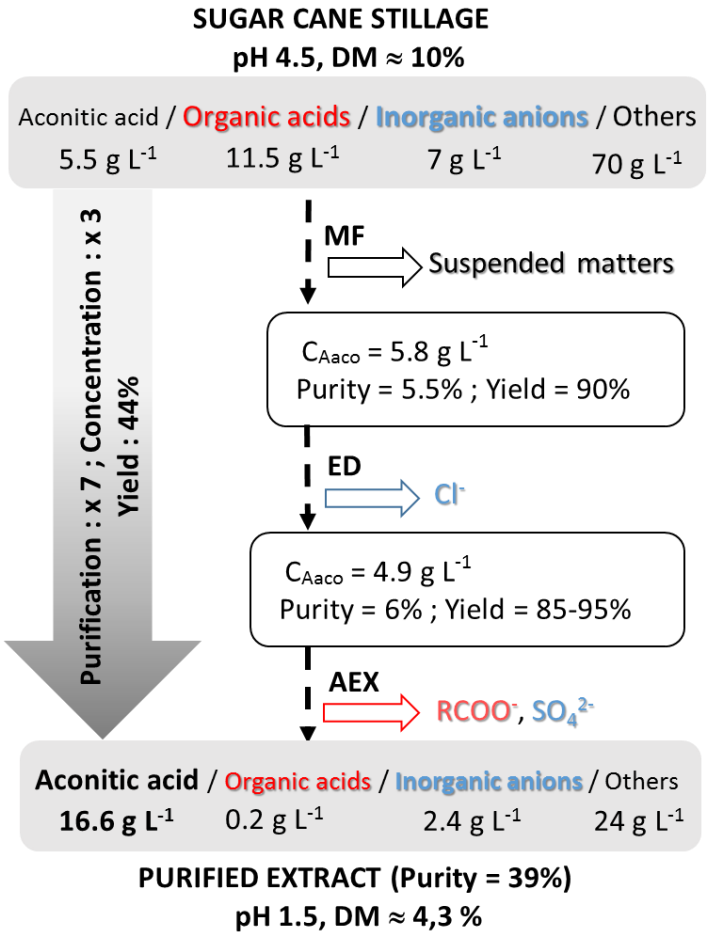

Figure 13. Overall purification process of aconitic acid from sugarcane stillage

Figures captions

Figure 1. Aconitic acid isomers and properties

Figure 2. Aconitic acid speciation diagram

Figure 3. Ion exchange isotherms on LEWATIT® S 4528 of aconitic acid with Cl^- and SO_4^{2-}. (a) Monovalent aconitate (H_2Aaco^-) for pH = 2.5-3.3; experimental and modeling (- - - - - K_x H_2Aaco^-/Cl^- = 5.7; ——— K_x H_2Aaco^-/SO_4^{2-} = 0.07); (b) Mixture of monovalent and divalent aconitate (Aaco) for pH = 4.1 - 5.6: experimental and modeling (——— K_x $Aaco/SO_4^{2-} \approx 5$). Comparison with experimental points for monovalent aconitate only.

Figure 4. Breakthrough curves of main components for the standard stillage (pH 4.5) on LEWATIT® S4528 resin in sulfate form (BV = 61.9 mL).

Figure 5. Experimental and simulated breakthrough curves for synthetic solution at pH 4.5 on LEWATIT® S4528 resin in (a) sulfate form; (b) chloride form.

(BV = 61 mL / 65 mL; x_{Aaco} = 0.2; x_{Sul} = 0.2; x_{Cl} = 0.6; N = 0.211 eq L^{-1}; Lines correspond to $D_{ax} = 10^{-5}$ m^2 s^{-1}; K_x Aaco/Cl = 5.3; K_x Aaco/Sul = 3.2 (then K_x Sul/Cl = 1.66)).

Figure 6. Experimental and simulated breakthrough curves for standard stillage at pH 4.5 on LEWATIT® S4528 resin in chloride form. (BV = 61.5 mL; x_{Aaco} = 0.18; x_{Sul} = 0.25; x_{Cl} = 0.57; N = 0.251 eq L^{-1}- ; Lines correspond to $D_{ax} = 10^{-5}$ m^2 s^{-1}; K_x Aaco/Cl = 5.3; K_x Aaco/Sul = 3.2 (then K_x Sul/Cl = 1.66)).

Figure 7. Experimental and simulated breakthrough curves at pH 3.6 on LEWATIT® S4528 resin in sulfate form for (a) the synthetic solution; (b) the standard stillage. (BV = 51.4 mL / 62.2 mL; x_{Aaco} = 0.13; x_{Sul} = 0.21 / 0.17; x_{Cl} = 0.66 / 0.7; N = 0.191 eq L^{-1}/ 0.196

eq L^{-1} ; Lines correspond to $D_{ax} = 10^{-5}$ m^2 s^{-1}; K_x Aaco/Cl = 3; K_x Aaco/Sul = 1.8 (K_x Sul/Cl = 1.66 unchanged)).

Figure 8. Elution curves of the main stillage components following a saturation step with standard stillage pH 4.5: (a) elution with H_2SO_4 0.5 N, for LEWATIT® S4528 initially under sulfate form; (b) elution with HCl 0.5 N, for LEWATIT® S4528 initially under chloride form. (BV = 61.7 mL; elution flow-rate = 1 BV h^{-1}).

Figure 9. Simulated breakthrough of aconitic acid contained in a synthetic solution with decreasing chloride content, at pH 4.5 on LEWATIT® S4528 resin in sulfate form. (Initial composition: $C_{Aaco\ F}$ = 5.01 g L^{-1}; $C_{Cl\ F}$ = 4.5 g L^{-1}; $C_{Sul\ F}$ = 1.91 g L^{-1} - Lines correspond to $D_{ax} = 10^{-5}$ m^2 s^{-1}; K_x Aaco/Cl = 5.3 ; K_x Aaco/Sul = 3.2 (then K_x Sul/Cl = 1.66)).

Figure 10. Simulation of the influence of the demineralization rate on the resin capacity for aconitic acid (chloride removal: resin in sulfate form; sulfate removal: resin in chloride form).

Figure 11. Evolution of the solutes retention rates in the diluate during electrodialysis (standard stillage – pH 4.5; U = 18 V; AMX and CMX NEOSEPTA membranes).

Figure 12. Experimental and simulated breakthrough curves at pH 4.5 on LEWATIT® S4528 resin in sulfate form for standard stillage after chloride removal by electrodialysis (BV = 49.8 mL; x_{Aaco} = 0.51; x_{Sul} = 0.44; x_{Cl} = 0.05; N = 0.088 eq L^{-1}; Lines correspond to $D_{ax} = 10^{-5}$ m^2 s^{-1}; K_x Aaco/Cl = 5.3 ; K_x Aaco/Sul = 3.2 (then K_x Sul/Cl = 1.66)).

Figure 13. Overall purification process of aconitic acid from sugarcane stillage